RSC Advances

ROYAL SOCIETY OF CHEMISTRY

www.rsc.org/advances

RSC Advances

ARTICLE

Side Chain Position, Length and Odd/Even Effects on 2D Self-Assembly of Mono-Substituted Anthraquinone Derivatives at Liquid/Solid Interface

Received 00th January 20xx,
Accepted 00th January 20xx

DOI: 10.1039/x0xx00000x

www.rsc.org/

Yi Hu, Kai Miao, Bao Zha, Xinrui Miao, Li Xu* and Wenli Deng*

The formation of self-assembled adlayers of 1-hydroxyanthraquinone (1-HA) and 2-hydroxyanthraquinone (2-HA) derivatives with various side chain length were investigated by scanning tunneling microscopy for the purpose of determining the influence of chemical structure on 2D molecular arrangement in self-assembly process. Different structures labeled as Linear I, Linear II, Linear III, Linear IV and Z-Like were presented based on their packing modes. Weak O···H-C hydrogen bonds existing between adjacent anthraquinone moieties are the key forces to drive the formation of ribbon A, A', B and C, which are the basic rows of the self-assembled stuctures. The emergence of odd or even number of carbon atoms in the alkyl chain induced structural diversity is an indication that one of the driving forces for 1-HA-OC_n (n = 15, 16) and 2-HA-OC_n (n = 12, 14–16) molecules to assemble into ordered 2D nanostructures is van der Waals interaction between interdigitated alkyl chains. 1-HA-OC_{16} and 1-HA-OC_{15} exhibited lamellar structures packed in Linear I and Linear II fashions. 2-HA-OC_{15} and 2-HA-OC_{16} adopted Linear III structures and Z-Like packing modes. Moreover, when the number of carbon atoms in side chain of 2-HA-OC_n molecules was decreased to 12, the self-assembled pattern could present a Linear IV phase. Notably, 2-HA-OC_{14} showed coexistence of Z-Like and Linear IV phases. Systematic experiments revealed that a better understanding of the alkyl chain position, length and odd/even effects on 2D self-assembly would shed light on better control of assembly patterns and design of new molecular materials.

Introduction

Massive research efforts are focusing on regulation of the arrangement of organic molecules on surfaces for developing novel functional materials.[1–5] Supramolecular two-dimensional (2D) structures on different substrates have attracted lots of attention for academic reasons as same as for their utility in wetting, lubrication, adhesion, adsorption and the fabrication of electronic and opto-electronic devices at the molecular scale.[6–8] As a consequence, there is significant financial motivation to generate a more predictive understanding of 2D crystal polymorphism. A powerful method to investigate the 2D organization of organic molecules by physisorption on surfaces is scanning tunneling microscopy (STM) at the liquid/solid interface, which provides information on structure and dynamics, offering submolecular resolution of both periodic and nonperiodic packing in a time-dependent fashion.[9–11] It is well-documented that successful monolayer formation and STM imaging require trimmed molecule–substrate, molecule–solvent and molecule–molecule interactions. Supramolecular structure is a result of the competition and balance between these interactions.[12,13] The nature of functional groups, the symmetrical characteristics, the number and position of the substituents, the length of alkyl chains, are the key factors deciding the chemical structures of molecules, and thus play a decisive role in the formation of self-assembled nanostructures. A large quantity of paper has reported the dependence of 2D supramolecular structures on alkyl chain length.[14–16] Much attention has been attached to the influence of odd or even number of carbon atoms in the side chains, which is a common phenomenon offering the alternate change of physical and chemical properties as well as crystalline structure of a molecule.[17–19] This side chain odd/even effect induced different self-assembly structures can be obviously observed when the formation of the 2D arrangement is dominated *via* van der Waals interactions between the alkyl chains, and it emerges as a result of the end methyl groups to minimize the steric repulsion.[17] Hydrogen bonds have been widely reported and explored for self-assembly purpose at liquid/solid interface and in three-dimensional crystals due to the relatively strong, selective and directional nature of hydrogen bonding interactions.[20] It can exert an influence on stabilizing self-assembled structures and weak O···H-C bonds have been widely reported in 2D crystal engineering.[21,22]

Kikkawa *et al.* has intensively explored the self-assemblies of bipyridine derivatives on highly oriented pyrolytic graphite (HOPG).

College of Materials Science and Engineering, South China University of Technology, Guangzhou 510640, China. E-mail: mslxu@scut.edu.cn, wldeng@scut.edu.cn; Tel: 86-20-22236708

Electronic Supplementary Information (ESI) available: Detailed description of experimental section and additional STM images. See DOI: 10.1039/x0xx00000x

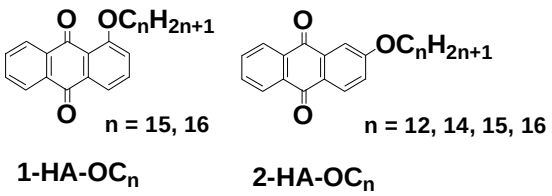

Scheme 1. Chemical structures of 1-hydroxyanthraquinone and 2-hydroxyanthraquinone derivatives.

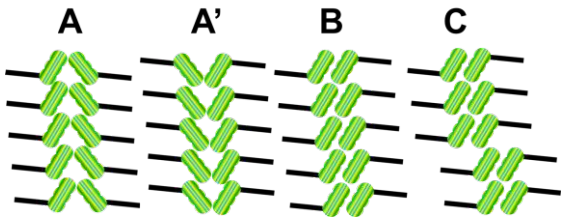

Figure 1. Four different aggregation modes of ribbon A, A', B and C. The anthraquinone cores and side chains are represented with green shapes and black lines, respectively.

proving fundamental insights into the role of the length, number and position of the substituents on molecular packing which is dominantly controlled by interactions between alkyl chains.[17,23,24] Isomeric tetrathienoanthracene derivatives have been reported not long ago.[25] Slight geometric difference between the two isomers, means position of sulphur atoms in the molecule, can lead to dramatic change in the monolayer structures.

Herein, we investigated the supramolecular structures of a series of 1-hydroxyanthraquinone and 2-hydroxyanthraquinone derivatives (Scheme 1) with mono-substituent side chains at liquid/solid HOPG interface with the help of STM. Through careful observation, different linear and Z-like structures were observed in the monolayers when the position or length of the alkyl chain changed. In one ribbon, molecules gathered in a head-to-head fashion *via* weak O···H-C hydrogen bonds, and then all of the ribbons form regular arrangement through alkyl chain interdigitation. In our research, the densely packed structures, which are entirely different from each other on their arrangement fashions, were compared and analysed in detail in order to explore how a slight chemical-structural change would influence self-assembly process and result in great difference on 2D molecular nanostructures.

The long alkyl chains show great commensurability with the graphite surface and are likely to arrange parallel to the substrate[26] and meanwhile force the π-conjugated anthraquinone moieties to firmly adsorb on HOPG. High-resolution STM images can reveal the apparent features of molecule packing fashions. We discovered that 1-HA-OC_{16} and 1-HA-OC_{15} showed totally different molecular arrangements, that is, Linear I and Linear II fashions, respectively. Not surprisingly, this is arisen from the different even and odd number of carbon atom in the alkyl chains. However, when the alkyl chain is in the 2-positon, another two kinds of self-assembly structures, namely, Linear III and Z-Like were generated for 2-HA-OC_{15} and 2-HA-OC_{16}, respectively. Besides, we obtained another linear structure called Linear IV for 2-HA-OC_{12}. 2-HA-OC_{14} adopted both Z-Like and Linear IV phases, indicating that the alkyl chain length played an important role in the self-assembled process. These results can better promote our understanding of the effect of side chain positon, length and odd or even property on 2D molecular self-assembly.

Experimental Section

1-Hydroxyanthraquinone (*n* = 15, 16) and 2-hydroxyanthraquinone (*n* = 12, 14–16) derivatives used in this study were synthesized as described in the supporting information (scheme S1), and then recrystallized repeatedly (four to six times) in order to ensure the purity of a high degree (≥98%). The solvent of 1-octanoic acid was purchased from Tokyo Chemical Industry without further purification. The solutions used in our work were under a concentration of 50% saturation. At first, 100% saturated solutions were prepared, and then they were diluted to 50% saturated according to accurate proportion. The samples were prepared by depositing a droplet (about 1μL) of solution on a freshly cleaved atomically flat surface of HOPG (quality ZYB, Bruker, USA). STM measurements were performed on a Nanoscope IIIa Multimode SPM (Bruker, USA) under ambient conditions with the tip immersed in the supernatant liquid. The tips were mechanically cut from Pt/Ir wires (80/20). All images were recorded with constant current mode and are shown without further processing. Tunneling parameters are given in the corresponding figure caption. Molecular models of the assembled structures were built using Materials Studio 4.4. The models were constructed based on the inter-molecular distances and angles, and analysis of the STM results. Also, they were tested to be right according to the ideal overlap with the high-resolution STM images. The DSC experiments were conducted with a scan rate of 10 °C/min for heating and cooling (Instrument: NETZSCH DSC 200F3). Room temperature and humidity were recorded to be 15 ~ 20 °C and 45 ~ 55%.

Results

1-HA-OC_n and 2-HA-OC_n molecules, consisting of π-conjugated anthraquinone moieties and alkyl chains, are expected to generate distinguish 2D nanostructures at the liquid/solid interface. Anthraquinone core substituted by a single alkyl chain in the 1-position and 2-position adopt completely different self-assembly patterns, which are constituted from four basic ribbon structures defined as ribbon A, A', B and C, as shown in Figure 1. All of the aggregation modes illustrate that the anthraquinone moieties stack with a regular sequence *via* a head-to-head fashion. For ribbon A and A', the anthraquinone portions arrange in a V-like shape, but during our experiments, careful observation proves that they are not mirror meristic. Ribbon A' is the same with ribbon A as the result of a rotation of 180°, but they represent different ribbon orientation in phases consist both of them. Nevertheless, in the case of ribbon B, the two rows of π-conjugated units are antiparallel to each other. Comparing with ribbon B, ribbon C shows regular dislocation of the antiparallel dimers, resulting in alternately aligned tetramers and hexamers.

In our present research, different kinds of 2D self-assembled networks were observed at the liquid/HOPG interface with 1-octanoic acid as the solvent under the same concentration of 50% saturation. No solvent coadsorption was observed, indicating that 1-octanoic acid exerted its function only as a dispersant.[27]

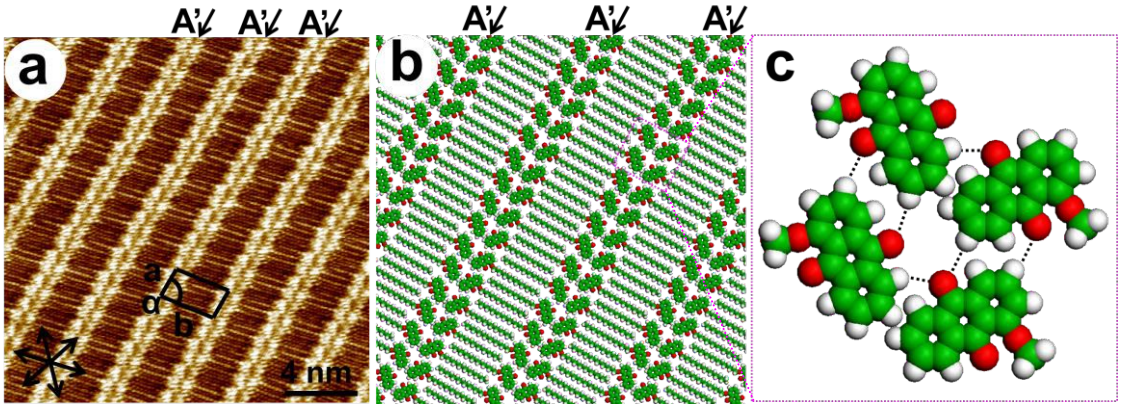

Figure 2. (a) High-resolution STM image of 1-HA-OC_{16} physisorbed at 1-octanoic acid/HOPG interface, showing the Linear I packing fashion. The black arrows indicate the 3-fold symmetry of HOPG substrate. (b) Molecular model for the lamellar structure. (c) Illustration of the O···H-C hydrogen bonds. The long alkyl chains are replaced by methyl groups. Imaging conditions: I_t = 500 pA, V_{bias} = 750 mV.

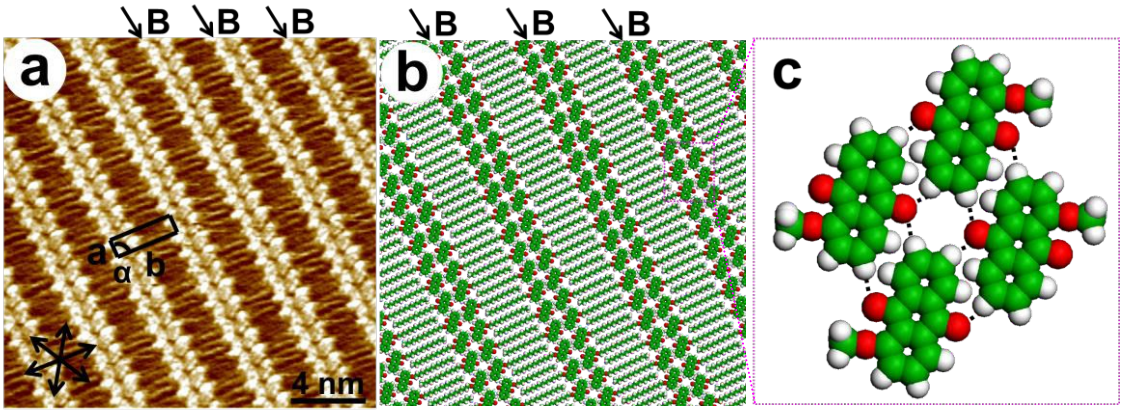

Figure 3. (a) High-resolution STM image of 1-HA-OC_{15} physisorbed at the 1-octanoic acid/HOPG interface, showing the Linear II packing fashion. The black arrows indicate the 3-fold symmetry of HOPG substrate. (b) Molecular model of the lamellar structure. (c) Illustration of the O···H-C hydrogen bonds. The long alkyl chains are replaced by methyl groups. Imaging conditions: I_t = 450 pA, V_{bias} = 600 mV.

Self-assembly of 1-HA-OC_{16}

Firstly, the 2D self-assembly of 1-HA-OC_{16} was explored. 1-HA-OC_{16} forms a linear structure on the HOPG surface, exhibiting a lamellar fashion (Figure 2 and S1), named as Linear I, which is constituted from ribbon A'. Figure 2a is the high-resolution STM image, showing the details of this self-assembled structure. The brighter rods and darker troughs represent anthraquinone moieties and alkyl chains, respectively, ascribing to higher electronic density for the former and lower for the latter.[27] It is obvious that all of the ribbons have the same orientation, and every ribbon consists of two rows of molecules which packed in a head-to-head and V-like mode. A set of arrows in the left bottom of Figure 2a is depicted, showing the main symmetry of HOPG under the monolayer. 1-HA-OC_{16} molecules arrange parallel to the substrate, with the alkyl chains extending along the main direction of the substrate. According to the molecular arrangement, a structural model is proposed in Figure 2b, corresponding well with the experimentally obtained STM images. Careful observation indicates that the ribbon is not mirror-symmetric. For this linear packing fashion, alkyl chains are supposed to be not fully interdigitated, means fifteen carbon atoms in a chain participate in the interdigitation between neighboring side chains, as shown in Figure S2. This dislocation by one atom is caused by the requirement for minimum steric repulsion, which is to be discussed in this paper. In this V-like ribbon, two rows of molecules are staggered tightly, through weak hydrogen bonds O···H-C in adjacent anthraquinone cores, as indicated in Figure 2c. The unit cell parameters for this Linear I arrangement can be defined with a = 0.8 ± 0.1 nm, b = 3.0 ± 0.1 nm and α = 86 ± 1°. Every unit cell consists of two molecules and the calculated area density is 1.20 nm² per molecule.

Self-assembly of 1-HA-OC_{15}

For the purpose of exploring how odd and even number of carbon atoms in the side chain can influence the 2D self-assembly process, we decreased the alkyl chain length of 1-HA-OC_n to n = 15. Figure 3a shows the high-resolution STM image of 1-HA-OC_{15} molecules adsorbed on HOPG surface. In the large-scale STM image of 1-HA-OC_{15} (shown in Figure S3), the HOPG surface is covered with orderly molecular adlayer, named as Linear II, which is constituted from the basic ribbon of B. The ribbon is composed of two molecular rows, which take a head-to-head and antiparallel configuration. The alkyl chains are arranged in an interdigitated way, leading to close

packing. The black arrows indicating the lattice direction of the graphite are superimposed in Figure 3a. The alkyl chains extend along the main direction of the substrate flatly, showing great matchability with the graphite lattice, and thus make the 1-HA-OC_{15} molecules tightly adsorb on the substrate surface through van der Walls interactions. A proposed structural model for this linear arrangement is depicted in Figure 3b and it is in good agreement with the STM results. Carbon atoms of neighboring chains tend to be arranged with each "up" atom in one chain next to a "down" atom in each of the two neighbors. This condition makes us come up with a guess that only fourteen carbon atoms in the alkyl chains of 1-HA-OC_{15} are alternated, instead of entirely alternated one (as shown in Figure S4). That is to say, highly matched structure can be achieved for 1-HA-OC_{15} molecules if the end methyl and the second methylene which is connected with the ether group in the adjacent two chains are pointing to the same direction. In order to minimize the steric repulsion, this shift by one atom along the side chain is reasonable and it will be systematically discussed in the discussion section. The weak hydrogen bonds O···H-C between two rows of anthraquinone moieties in a ribbon are illustrated in Figure 3c. A unit cell for this linear structure is outlined with the parameters of a = 1.0 ± 0.2 nm, b = 3.3 ± 0. 2 nm and α = 84 ± 2°. Every unit cell consists of two molecules and the calculated area density is 1.64 nm² per molecule.

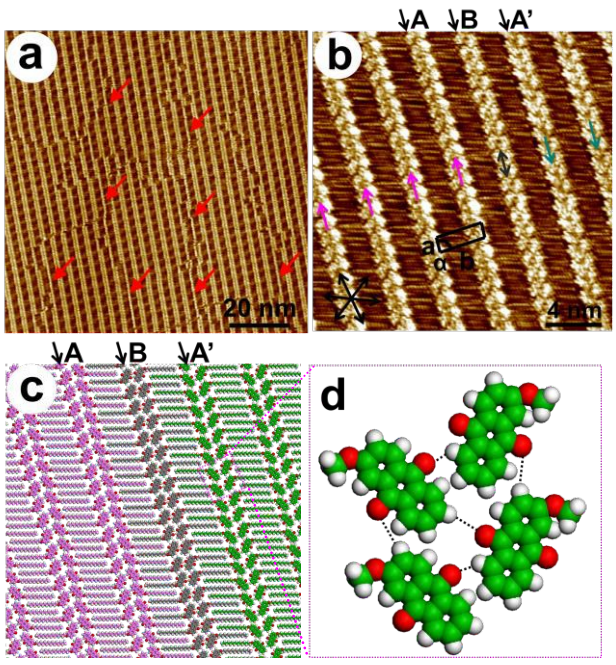

Figure 4. (a) Large-scale and (b) high-resolution STM images of 2-HA-OC_{15} physisorbed at 1-octanoic acid/HOPG interface, showing the Linear III packing fashion. The pink and green arrows in (b) represent the direction of V-like ribbons in different domains. The black arrows in the bottom left of (b) indicate the 3-fold symmetry of HOPG substrate. (c) Molecular model for the lamellar structure. (d) Illustration of the O···H-C hydrogen bonds. The long alkyl chains are replaced by methyl groups. Imaging conditions: I_t = 550 pA, V_{bias} = 800 mV.

Self-assembly of 2-HA-OC_{15}

In the case of 2-HA-OC_n derivatives, different linear structures were observed, which are powerful evidence for the importance of the substituent position on molecular self-assembly process. Figure 4a is the large-scale STM image for 2-HA-OC_{15} on HOPG surface. Except for some disconnected single rows, as marked by red arrows, which occur by chance, the adlayer consists of three kinds of ribbons means ribbon A, A' and B. This linear arrangement, defined as Linear III, can also be considered as a combination of two domains one domain made up from ribbon A and another made up from ribbon A'. These domains are orienting to reverse direction, as noted by pink and green arrows for ease of distinction. Ribbon B is seldom to be found and it is just a needed interim ribbon, guaranteeing smooth transition between the reverse domains, instead of the occurrence of unstable domain boundaries. A set of black arrows in Figure 4b indicate the lattice direction of the graphite, and the alkyl chains extend along the symmetry axis of the substrate. Alkyl chains are fully interdigitated with each other through van der Walls interactions and two rows of molecules in a ribbon are staggered via hydrogen bonds. The unit cell parameters for this linear arrangement are a = 1.1 ± 0.3 nm, b = 3.0 ± 0. 3 nm and α = 88 ± 3°. Every unit cell consists of two molecules and the calculated area density is 1.65 nm² per molecule. Figure 4d is an illustration of weak hydrogen bonds O···H-C between two rows of the ribbons.

Self-assembly of 2-HA-OC_{16}

Odd or even number of the carbon atoms in side chains can immensely affect the self-assembly structure, and this phenomenon has also been found when the substituent group is in the 2-position. 2-HA-OC_{16} molecules form a Z-like adlayer, named as Z-Like, in which the anthraquinone moieties arrange in a zigzag shape. The basic ribbon is ribbon C. Figure 5a is the STM image for a large area. Several obvious single rows indicated by red arrows, which appear randomly and destroy the uniformity of the adlayer, can be regarded as accidental circumstance. Figure 5b is the high-resolution STM image of 2-HA-OC_{16}, showing detailed packing information for this non-straight linear structure. The black arrows in the bottom left of Figure 5b indicate the main symmetry of the HOPG. The long alkyl chains show good commensurability with the graphite surface in order to maximize the adsorbate–substrate interaction. On the basis of STM results, a structural model for this Z-Like packing fashion is proposed, as shown in Figure 5c, which matches well with the observed molecules. A unit cell is presented on the image of Figure 5b with a = 4.6 ± 0.2 nm, b = 3.7 ± 0.2 nm and α = 73 ± 1°. The unit cell consists of ten molecules and the calculated area density is 1.63 nm² per molecule. This Z-Like arrangement is similar with the Linear II structure for 1-HA-OC_{15}, that is to say, the former can be regarded as the result of a one molecule-dislocation from the latter for every two or three dimers, along the alkyl chain direction. As a result, tetramers and hexamers are formed. Careful observation discovered that there is no disciplinary emergence for tetramers and hexamers in a Z-like ribbon, for instance, tetramer-hexamer-tetramer-hexamer arrangement, but the adjacent ribbons arrange in a perfectly dense packing fashion. The weak hydrogen bonds O···H-C in tetramer and hexamer aggregations are illustrated in Figure 5d.

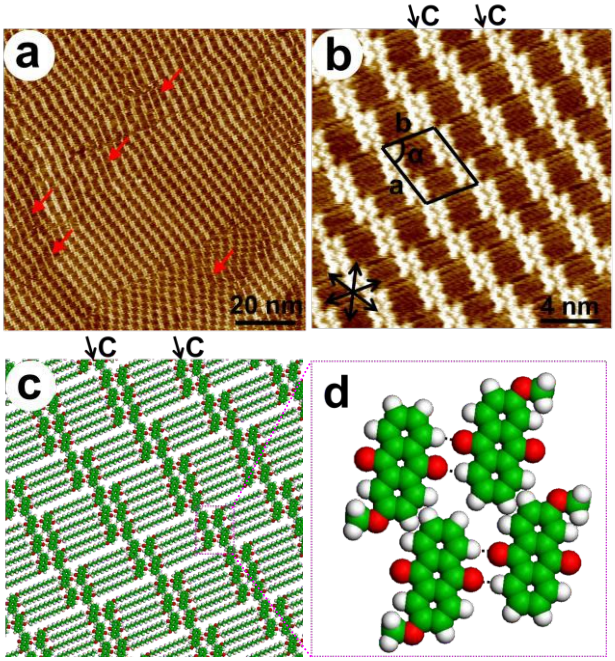

Figure 5. (a) Large-scale and (b) high-resolution STM images of 2-HA-OC_{16} physisorbed at 1-octanoic acid/HOPG interface, showing the Z-Like packing fashion. The black arrows in the bottom left of (b) indicate the 3-fold symmetry of HOPG substrate. (c) Proposed molecular model for the Z-Like structure. (d) Illustration of the O···H-C hydrogen bonds. The long alkyl chains are replaced by methyl groups. Imaging conditions: I_t = 450 pA, V_{bias} = 650 mV.

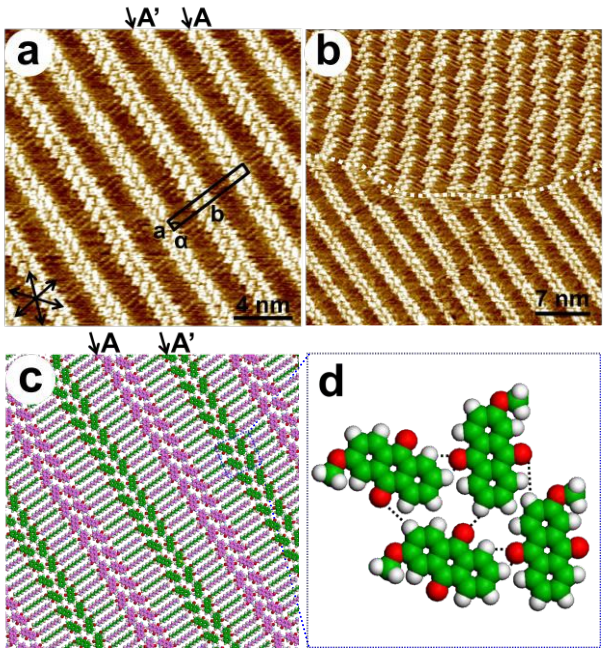

Figure 6. (a) High-resolution STM image of 2-HA-OC_{12} physisorbed at 1-octanoic acid/HOPG interface, showing the Linear IV arrangement. The black arrows in the bottom left indicate the 3-fold symmetry of HOPG substrate. (b) STM image of 2-HA-OC_{12} physisorbed on HOPG surface, showing the coexistence of Linear IV and Z-Like phases. (c) Molecular model for the Linear IV structure of 2-HA-OC_{12}. V-like ribbon A and A' are reversed to each other, and they are modeled in different colors for ease of distinction. (d) Illustration of the O···H-C hydrogen bonds. The long alkyl chains are replaced by methyl groups. Imaging conditions: I_t = 600 pA, V_{bias} = 800 mV.

Self-assembly of 2-HA-OC_{12} and 2-HA-OC_{14}

As a step further, we decreased the alkyl chain length of 2-HA-OC_n to n = 12 and 14, with the purpose of understanding chain length effect on self-assembly. Another linear structure labeled as Linear IV was observed. From a large-scale STM image for 2-HA-OC_{12} (Figure S5), it can be clearly seen that the 100 × 100 nm^2 area is not uniform, which consists of several domains with distinct boundaries. Figure 6a is the high-resolution STM image, exhibiting careful assembly information. The Linear IV arrangement is constituted by regularly staggered V-like ribbons of A and A'. The unit cell parameters are a = 0.8 ± 0.3 nm, b = 5.9 ± 0.3 nm and α = 89 ± 2°. Every unit cell consists of four molecules and the calculated area density is 1.18 nm^2 per molecule. The alkyl chains all extend along the same direction (the lattice direction of the graphite, as the black arrows in Figure 6a shown), parallel to each other and are fully interdigitated. On the basis of large amount of high-resolution STM images, a structural model for this Linear IV packing fashion is proposed in Figure 6c, which is in good consistent with the experimental results. V-like ribbons of A and A' are reversed to each other but with the same visual appearance. Two rows of molecules are arranged regularly through hydrogen bonds, which are illustrated in Figure 6d. Interestingly, 2-HA-OC_{14} molecules self-assemble into a monolayer consists of both Linear IV and Z-Like phases, as shown in Figure 6b and S6. The basic unit cells are imposed in Figure S6b and Figure S6c with the parameters of a = 0.9 ± 0.1 nm, b = 6.3 ± 0.1 nm, α = 84 ± 1° for Linear IV structure and a = 5.5 ± 0.2 nm, b = 3.6 ± 0.2 nm, α = 67 ± 2° for Z-Like structure. According to the unit cell parameters, the calculated area density are greatly different, namely, 1.41 nm^2 per molecule for Linear IV pattern and 1.82 nm^2 per molecule for Z-Like network. Then we can conclude that the Linear IV structure is denser than the Z-Like structure. That is to say, as the alkyl chain length decreases, 2-HA-OC_n molecules form Z-Like (n = 16), Z-Like and Linear IV (n = 14), Linear IV (n = 12) phases, respectively, which can be attributed to chain-length effect.

Discussion

Table 1 systematically summarizes the linear and Z-like structures from several aspects of basic packing fashion, shape, unit cell parameters, geometric characteristics and molecular density. The monolayer morphology is governed by the chemical structure, and both of 1-HA-OC_n and 2-HA-OC_n molecules showed great dependence on the side chain position, length and odd/even effect. Therefore, the 2D self-assembly of anthraquinone derivatives can be tuned by efficiently changing properties of the alkyl chains. For better understanding the relationships and easy comparison of Linear I, Linear II, Linear III, Linear IV and Z-Like configurations, we made a graphical summary of structural model, as shown in Figure 7.

On the basis of the STM analysis, the 2D structure formation for 1-HA-OC_n and 2-HA-OC_n derivatives is dominated by (i) hydrogen bonds of the anthraquinone units, (ii) intermolecular van der Waals

Table 1. Schematic unit cell parameters and other characteristic parameters of the different structures observed in 2D self-assembly monolayers

molecule	structure	basic ribbon	ribbon shape	unit cell parameters			N [a]	S (nm^2) [b]
				a (nm)	b (nm)	α (°)		
1-HA-OC$_{16}$	Linear I	A'	V-like	0.8 ± 0.1	3.0 ± 0.1	86 ± 1	2	1.20
1-HA-OC$_{15}$	Linear II	B	antiparallel	1.0 ± 0.2	3.3 ± 0.2	84 ± 2	2	1.64
2-HA-OC$_{15}$	Linear III	A, A', B	V-like and antiparallel	1.1 ± 0.3	3.0 ± 0.3	88 ± 3	2	1.65
2-HA-OC$_{16}$	Z-Like	C	antiparallel	4.6 ± 0.2	3.7 ± 0.2	73 ± 1	10	1.63
2-HA-OC$_{14}$	Z-Like	C	antiparallel	5.5 ± 0.2	3.6 ± 0.2	67 ± 2	10	1.82
	Linear IV	A, A'	V-like	0.9 ± 0.1	6.3 ± 0.1	84 ± 1	4	1.41
2-HA-OC$_{12}$	Linear IV	A, A'	V-like	0.8 ± 0.3	5.9 ± 0.3	89 ± 2	8	1.18

[a] N = number of molecules per unit cell. [b] S represents the area density.

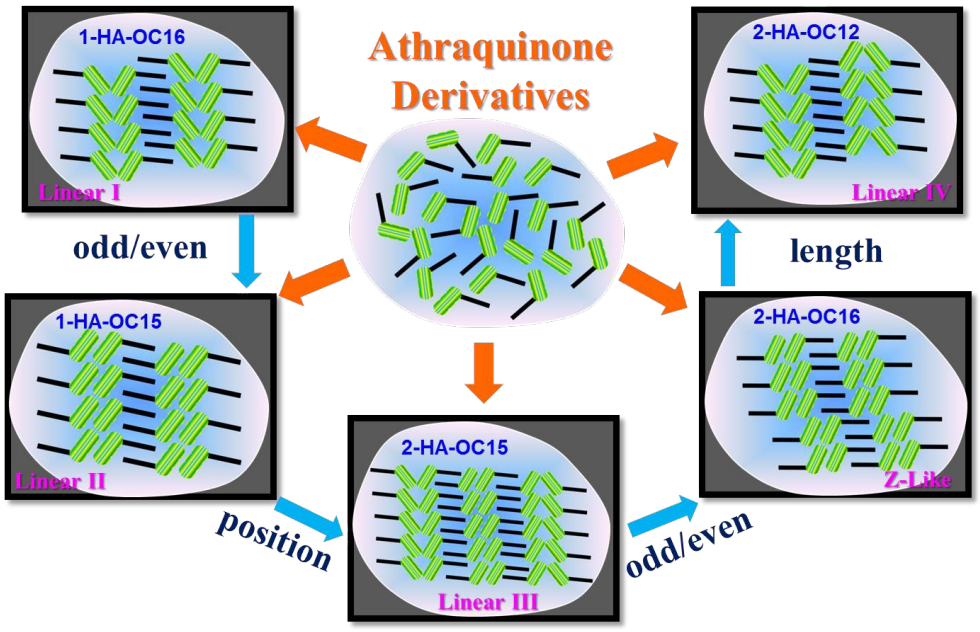

Figure 7. Schematic representation for self-assembled Linear I, Linear II, Linear III, Linear IV and Z-Like structures. The anthraquinone cores and side chains are represented with green shapes and black lines, respectively.

interactions of the alkyl chains, and (iii) molecule–substrate interactions. Adjacent molecules in ribbon A, A', B and C are staggered *via* weak hydrogen bonds between π-conjugated anthraquinone moieties (i). Ribbons are arranged mutually by alkyl chain interdigitation (ii). The monolayer adsorbed tightly on the HOPG surface by interplay between the adsorbate and substrate (iii).

Weak hydrogen bonding interactions between anthraquinone units

Weak hydrogen bonds can direct the formation of 2D crystalline structures[28] and molecular recognition process, ascribing to their high directionality. For 1-HA-OC$_n$ and 2-HA-OC$_n$ derivatives, weak O···H-C hydrogen bonds are found, with the carbonyl oxygen as an acceptor and hydrogen in the adjacent anthraquinone moieties as a donor. This type of hydrogen bonds have been reported before.[21,22] Moreover, similar weak hydrogen bonds formed between anthraquinone units have been reported by Tamaki *et al.*[29] Hydrogen atom in the benzene ring has the ability to form O···H hydrogen bonds[30,31], which will, as a consequence, significantly impact the 2D self-assembly formation.

In our research, the π-conjugated anthraquinone units in ribbon A, A', B and C are arranged into two fashions, V-like and antiparallel pattern, and they gathered with each other not only through the common van der Waals interactions, but also *via* weak hydrogen bonds, as shown in Figure 2c, 3c, 4d, 5d and 6d. It is w

known that molecules under a given ambient condition favor assembled structures which are as denser as possible. Upon comparing the molecule density of 1-HA-OC_{15} and 2-HA-OC_{15}, we found that their compact degree were nearly the same, namely, 1.64 nm² per molecule for 1-HA-OC_{15} and 1.65 nm² per molecule for 2-HA-OC_{15} (as the *S* value indicated in Table 1). As a consequence, we conclude that close-packed structures can be obtained whether through weak hydrogen bonds induced V-like or antiparallel combination modes. However, 2-HA-OC_{16} showed lower molecule density (1.63 nm² per molecule) than 1-HA-OC_{16} (1.20 nm² per molecule), indicating that dimer dislocation in a ribbon along the direction of the alkyl chains would cause the decrease of compact degree.

Side chain position induced different self-assemblies

Chemical structure is one of the crucial factors on dominating the formation of 2D molecular self-assembly networks on solid substrate and thus can be utilized for purpose of desirable surface patterns.[27,32–34] Change of the alkyl chain position from position 1 to 2 resulted in tremendous variation for physical properties as well as for self-assembly structures. Figure 8a is the differential scanning calorimetry (DSC) thermograms of 1-HA-OC_n (*n* = 15, 16) and 2-HA-OC_n (*n* = 12, 14−16). In addition, a series of 1-HA-OC_n and 2-HA-OC_n (*n* = 11 to 18) compounds were synthesized in order to get enough DSC data and then summarize the transformation regularity as the position, length and odd or even number of side chain change (Figure S7). 1-HA and 2-HA derivatives show gradually changed phase-transition temperature (obtained from differential scanning calorimetry testing, on the trace of heating), which are assigned to the melting point. In Figure 8b, the blue line is above the red line, demonstrating that the melting point for 1-HA-OC_n is higher than that for 2-HA-OC_n. This significant increase of phase-transition temperature can be ascribed to the relatively large energy required to form an isotropous and clear phase from the solid state in ambient condition.[35,36] Therefore, we can conclude that 1-HA-OC_n and 2-HA-OC_n derivatives need quite different energy for self-assembling into ordered 2D formation, thus different kinds of structures are formed, which are stable both thermodynamically and kinetically.

Effect of odd or even number of the side chain on 2D self-assembly

Whether the number of carbon atoms in the side chains is odd or even has also been well-known to affect the properties of organic molecules and their packing fashions at liquid/solid interface. It can be evidently seen that the melting point of both 1-HA-OC_n and 2-HA-OC_n derivatives increase in an up-down-up-down tendency, as the zigzag lines demonstrated, corresponding to the odd-even-odd-even number of the carbon atoms (Figure 8b). The structural difference induced by odd or even number of carbon atoms in the alkyl chain is proposed as a result of the requirement for the end methyl group to minimize the steric repulsion, and its appearance to the system is an indication that the major driving force of the 2D structural formation is intermolecular interplay of alkyl chains. 1-HA-OC_{15} and 1-HA-OC_{16}, or 2-HA-OC_{15} and 2-HA-OC_{16} adopted distinguish assembled patterns, owing to making the van der Waals interactions between the side chains reach the maximum comfort

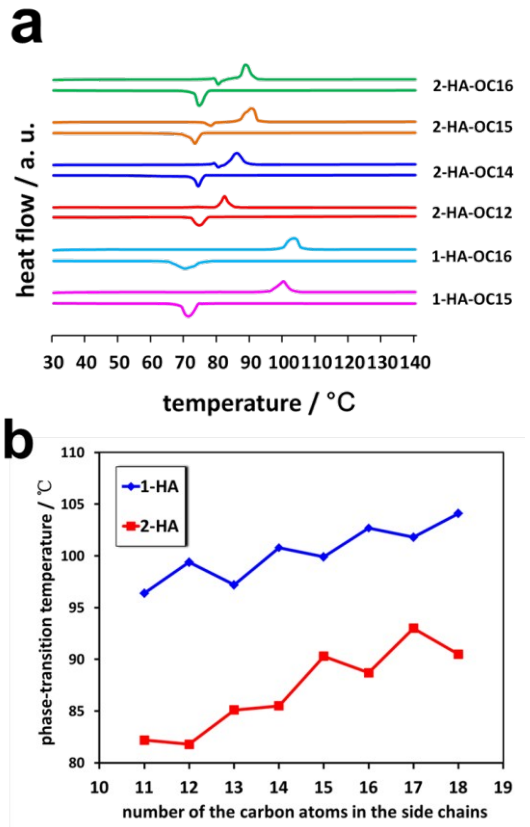

Figure 8. DSC thermograms of compounds 1-HA-OC_n (*n* = 15, 16) and 2-HA-OC_n (*n* = 12, 14−16) for the trace of heating (the above line) and cooling (the below line). (b) Dependence of the phase-transition temperature (melting point) for 1-HA-OC_n and 2-HA-OC_n (*n* = 11−18) derivatives on the number of carbon atoms in the side chains.

and energetic equilibrium. Carbon atoms of neighboring chains should be staggered, with each "up" atom in one chain next to a "down" atom in each of the two neighbors, in order to get dense 2D packing on surface.[37] Therefore, this condition can be achieved by 1) atom shift, resulting in partially interdigitated alkyl chains, for example, Linear I and Linear II packing fashions. 2) Molecule rotation of 180°, resulting in opposite ribbon direction, such as the Linear IV phase.

Even though STM cannot observe the interdigitated alkyl chains to high accuracy of single atoms, we suppose that side chains of 1-HA-OC_{15} and 1-HA-OC_{16} molecules are partially interdigitated. Figure 9 shows the space filling of the matched methyl and methylene groups in the side chains with pink arrows indicating the "down" direction and blue arrows indicating the "up" direction. Orange and yellow rectangles represent the repulsive and matched carbon atoms in the neighboring side chains, respectively. Fully interdigitated alkyl chains are favored in consideration of close packing. However, in our research, we guessed that partially interdigitated ones are more reasonable for 1-HA-OC_{15} and 1-HA-OC_{16} molecules. In Linear I packing fashion for 1-HA-OC_{16}, if alkyl chains are fully interdigitated, as shown in Figure 9a, the adjacent carbon atoms in neighboring side chains will point to reverse direction, and this repulsive condition can result in great steric

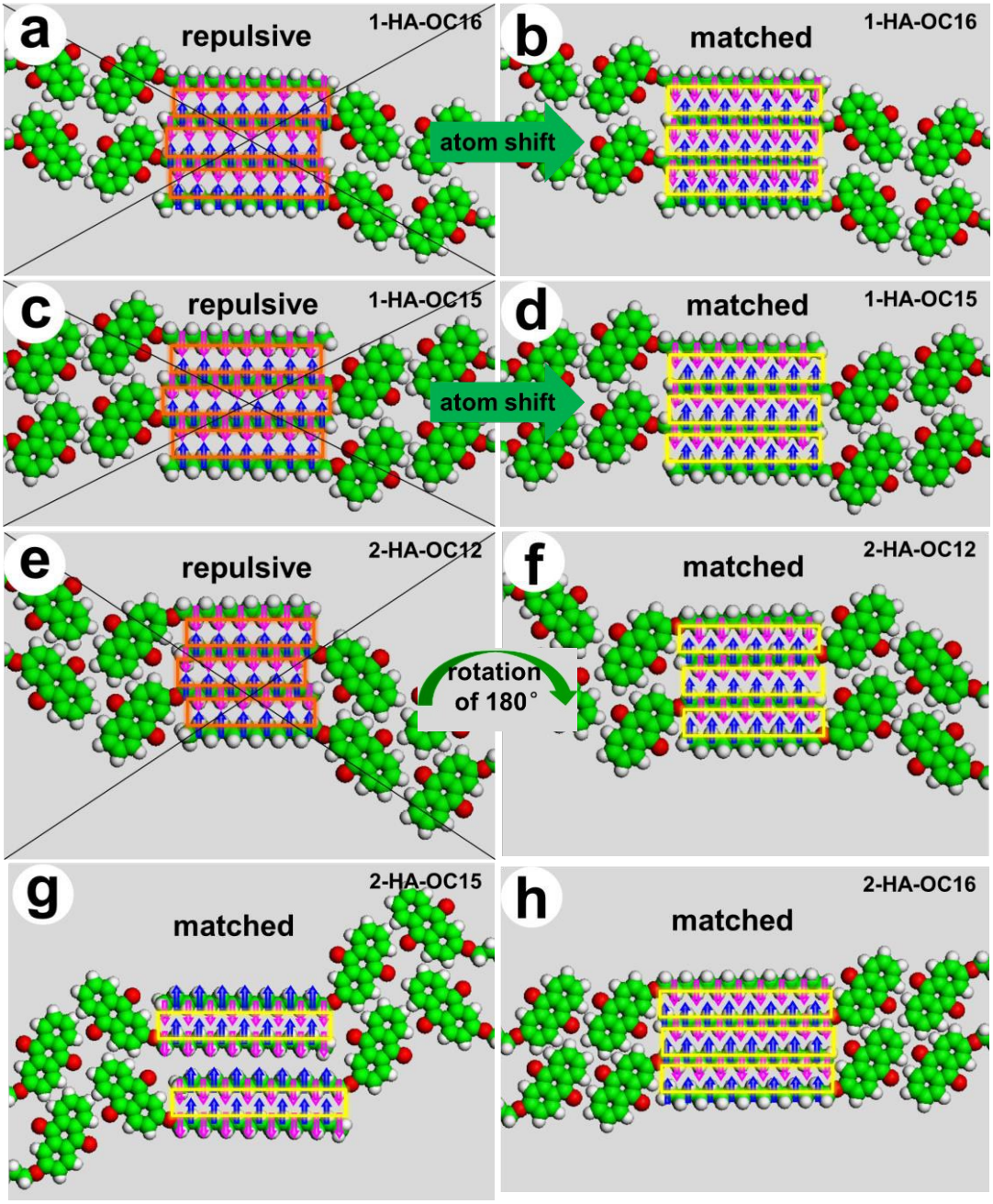

Figure 9. Space-filling spheres figure representation of the matched methyl and methylene groups in the side chains with pink arrows indicating the "down" direction and blue arrows indicating the "up" direction. Orange and yellow rectangles represent the repulsive and matched carbon atoms in the neighboring side chains, respectively. (a and c) Assumed fully interdigitated models for 1-HA-OC_{16} and 1-HA-OC_{15}. (b and d) Reasonable models for 1-HA-OC_{16} and 1-HA-OC_{15} with partially interdigitated alkyl chains in consideration of steric repulsion. (e) Assumed model for 2-HA-OC_{12} with the adjacent ribbons direct to the same direction. (f–h) Proposed models on base of STM results with fully interdigitated alkyl chains and minimum steric repulsion.

repulsion. However, in the case of partially interdigitated condition as shown in Figure 9b, which can be achieved by one atom shift, alkyl chains are highly matched and this condition is more reasonable. Therefore, we assume that only fifteen carbon atoms in the alkyl chains of 1-HA-OC_{16} are alternated. Similarly, for the Linear II packing fashion of 1-HA-OC_{15}, fourteen carbon atoms in a chain participate in the interdigitation between neighboring side chains (Figure 9d), instead of fully interdigitated one (Figure 9c). This shift by one atom is also caused by the requirement for minimum steric repulsion. Our STM results indicate that in Linear IV packing fashion for 2-HA-OC_{12}, the adjacent V-like ribbons point to the opposite direction (as shown in Figure 9f), and as a result, carbon atoms of neighboring chains are staggered, with each "up" atom in one chain matches well with the next "down" atom in each of the two neighbors. Compared with another condition we assumed in Figure 9e, in which ribbons of 2-HA-OC_{12} are pointing to the same direction

and then neighboring carbon atoms are repulsive to each other, we affirm that this rotation of 180° is needed for the purpose of minimizing steric repulsion. Besides, in the case of Linear III structure for 2-HA-OC_{15} (Figure 9g) and Z-Like structure for 2-HA-OC_{16} (Figure 9h), no atom shift or molecule rotation are needed, because these kinds of fully interdigitated fashions reach ideally dense packing and minimum steric repulsion.

Side chain length induced structural difference for 2-HA-OC_n (*n* = 12, 14, 16)

Dependence of 2D supramolecular structures on alkyl chain length is a common phenomenon. On the basis of STM observation, we found that 2-HA-OC_n derivatives displayed apparent structural difference when the alkyl chain is shortened from 16 to 12. 2-HA-OC_{16} favored a packing fashion of Z-Like, 2-HA-OC_{12} adopted the 2D nanopattern of Linear IV, but 2-HA-OC_{14} displayed a configuration of coexistent Z-Like and Linear phases (see Figure 6b, S6b and S6c). Then a question arises why the gradually decreased alkyl chain length can lead to related structural change. According to the unit cell parameters shown in Table 1, the calculated area density for Linear IV and Z-Like patterns of 2-HA-OC_{14} are greatly different, namely, 1.41 nm^2 per molecule for Linear IV and 1.82 nm^2 per molecule for Z-Like. Then we can conclude that the Linear IV structure is denser than the Z-Like structure. It is well-known that the 2D self-assembly structures at the liquid/solid interface involve a balance and competition between adsorption and desorption of the solute molecules.[38] The adsorption of molecules from the solution is under kinetic control.[39] As the CH_2 units for side chains decrease, the van der Walls interactions between the solvent and solute molecules decrease. Therefore, the number of molecules adsorbed from the solution onto the surface per area and time increases monotonically with the decrease of the side chain length[21], and thus favors the formation of Linear IV with denser area density.

Conclusion

STM observation of 1-HA-OC_n and 2-HA-OC_n molecules was performed at liquid/solid interface. Different linear and Z-like self-assembly patterns called Linear I, Linear II, Linear III, Linear IV and Z-Like were found, by changing the chemical structures. Two molecular rows in each ribbon aggregated with each other by weak O···H-C hydrogen bonds between π-conjugated anthraquinone moieties and formed head-to-head arrangement modes. In the lamellas, ribbons gathered together *via* alkyl chain interdigitation. Careful analysis of the experimental unit cell parameters for 1-HA-OC_{15} and 2-HA-OC_{15} allows us to draw a conclusion that V-like and antiparallel combination style for anthraquinone moieties have the similar packing density, while dislocation which may result in Z-like ribbon can lead to less denser molecular arrangement. Linear I and Linear II, Linear III and Z-Like patterns were induced by odd/even property of the side chains. Linear I and Z-Like, Linear II and Linear III structures were different, ascribing to different side chain position. Besides, the difference between Z-Like and Linear IV configurations was caused by alkyl chain length. These results showed that position of the substituent, length of the alkyl chain and the odd or even number of carbon atoms in the side chain can immensely affect the packing fashions of different adlayers, and thus should be taken into account on regulating 2D molecular self-assembly nanostructures.

Acknowledgements

Financial supports from the National Program on Key Basic Research Project (2012CB932900), the National Natural Science Foundation of China (51373055, 21403072, 21573077), the China Postdoctoral Science Foundation (2014M552189), and the Fundamental Research Funds for the Central Universities (SCUT) are gratefully acknowledged.

Notes and references

1 C. Marie, F. Silly, L. Tortech, K. Müllen, D. Fichou, *ACS Nano,* 2010, **4**, 1288−1292.
2 J. A. Elemans, I. De Cat, H. Xu, S. De Feyter, *Chem. Soc. Rev.*, 2009, **38**, 722−736.
3 L. Piot, F. Silly, L. Tortech, Y. Nicolas, P. Blanchard, J. Roncali, D. Fichou, *J. Am. Chem. Soc.*, 2009, **131**, 12864−12865.
4 J. F. Dienstmaier, K. Mahata, H. Walch, W. M. Heckl, M. Schmittel, M. Lackinger, *Langmuir,* 2010, **26**, 10708−10716.
5 F. P. Cometto, K. Kern, M. Lingenfelder, *ACS Nano,* 2015, **9**, 5544−5550.
6 F. Tao, S. L. Bernasek, *Chem. Rev.*, 2007, **107**, 1408−1453.
7 H. B. Fang, L. C. Giancarlo, G. W. Flynn, *J. Phys. Chem. B,* 1998, **102**, 7421−7424.
8 D. M. Cyr, B. Venkataraman, G. W. Flynn, *Chem. Mater.,* 1996, **8**, 1600−1615.
9 X. Y. Yang, X. Dou, A. Rouhanipour, L. J. Zhi, H. J. Räder, K. Müllen, *J. Am. Chem. Soc.*, 2008, **130**, 4216−4217.
10 H. Zhou, H. Dang, J. H. Yi, A. Nanci, A. Rochefort, J.D. Wuest, *J. Am. Chem. Soc.*, 2007, **129**, 13774−13775.
11 S. S. Li, H. J. Yan, L. J. Wan, H. B. Yang, B. H. Northrop, P. J. Stang, *J. Am. Chem. Soc.*, 2007, **129**, 9268−9269.
12 F. Tao, S. L. Bernasek, *Langmuir*, 2007, **23**, 3513−3522.
13 S. De Feyter, F. C. De Schryver, *J. Phys. Chem. B* 2005, **109**, 4290−4302.
14 Y. Miyake, T. Nagata, H. Tanaka, M. Yamazaki, M. Ohta, R. Kokawa, T. Ogawa, *ACS Nano*, 2012, **6**, 3876−3887.
15 X. Shao, X. C. Luo, X. Q. Hu, K. Wu, *J. Phys. Chem. B* 2006, **110**, 15393−15402.
16 K. Tahara, K. Inukai, N. Hara, C. A. Johnson II, M. M. Haley, Y. Tobe, *Chem. Eur. J.,* 2010, **16**, 8319–8328.
17 Y. Kikkawa, E. Koyama, S. Tsuzuki, K. Fujiwara, M. Kanesato, *Langmuir,* 2010, **26**, 3376−3381
18 F. Tao, J. Goswami, S. L. Bernasek, *J. Phys. Chem. B* 2006, **110**, 4199−4206..
19 L. Xu, X. R. Miao, B. Zha, K. Miao, W. L. Deng, *J. Phys. Chem. C*, 2013, **117**, 12707−12714.
20 K. S. Mali, K. Lava, K. Binnemans, S. De Feyter, *Chem. Eur. J.*, 2010, **16**, 14447–14458.
21 L. Kampschulte, M. Lackinger, A. K. Maier, R. S. K. Kishore, S. Griessl, M. Schmittel, W. M. Heckl, *J. Phys. Chem. B* 2006, **110**, 10829–10836.
22 L. Kampschulte, T. L. Werblowsky, R. S. K. Kishore, M. Schmittel, W. M. Heckl, M. Lackinger, *J. Am. Chem. Soc.,* 2008, **130**, 8502–8507.
23 Y. Kikkawa, E. Koyama, S. Tsuzuki, K. Fujiwara, K. Miyake, T. Tokuhisa, M. Kanesato, *Surf. Sci.*, 2007, **601**, 2520–2524.

24 Y. Kikkawa, E. Koyama, S. Tsuzuki, K. Fujiwara, K. Miyake, H. Tokuhisa, M. Kanesato, *Chem. Commun.*, 2007, **13**, 1343–1345.
25 C. Fu, F. Rosei, D.F. Perepichka, *ACS Nano*, 2012, 6, 7973–7980.
26 J. P. Rabe, S. Buchholz, *Science (New York, N.Y.)*, 1991, **253**, 424–427.
27 X. Zhang, Q. Chen, G. J. Deng, Q. H. Fan, L. J. Wan, *J. Phys. Chem. C* 2009, **113**, 16193–16198.
28 Ciesielski, C. A. Palma, M. Bonini, P. Samori, *Adv. Mater.,* 2010, **22**, 3506–3520.
29 T. Yoshinori, M. Kosuke, M. Kazuo, *B. Chem. Soc. JPN.*, 2013, **86**, 354–362.
30 Meier, U. Ziener, K. Landfester, P. Weihrich, *J. Phys. Chem. B*, 2005, **109**, 21015–21027.
31 Z. C. Mu, L. J. Shu, H. Fuchs, M. Mayor, L. F. Chi, *J. Am. Chem. Soc.*, 2008, **130**, 10840–10841.
32 L. J. Wan, *Accounts Chem. Res.*, 2006, **39**, 334–342.
33 J. V. Barth, Annu. *Rev. Phys. Chem*., 2007, **58**, 375–407.
34 S. S. Li, B. H. Northrop, Q. H. Yuan, L. J. Wan, P. J. Stang, *Accounts Chem. Res*., 2009, **42**, 249–259.
35 J. Y. Wang, J. Yan, L. Ding, Y. Ma, J. Pei, *Adv. Funct. Mater.*, 2009, **19**, 1746–1752.
36 L. Y. Park, D. G. Hamilton, E. A. McGehee, K. A. McMenimen, *J. Am. Chem. Soc.,*2003, **125**, 10586–10590.
37 K. G. Nath, O. Ivasenko, J. A. Miwa, H. Dang, J. D. Wuest, A. Nanci, D. F. Perepichka, F. Rosei, *J. Am. Chem. Soc.,* 2006, **128** 4212–4213.
38 Y. B. Li, Z. Ma, G. C. Qi, Y. L. Yang, Q. D. Zeng, X. L. Fan, C. Wang, W. Huang, T *J. Phys. Chem. C*, 2008, **112**, 8649–8653.
39 L. Xu, X. R. Miao, L. H. Cui, P. Liu, X. F. Chen, W. L. Deng *Nanoscale,* 2015, **7**, 11734–11745.